# 1 Preliminary Concepts

In this chapter we look at some physics of particle and radiation beams in the paraxial approximation. A *paraxial* beam is one that is well-collimated along its propagation direction, which we take to be the $z$ axis. For a relativistic electron beam to be paraxial means that the angle between $\hat{z}$ and the velocity vector of a typical electron is small, so that $v_z \gg |\boldsymbol{v}_\perp|$ and $v_z \approx c$. In the case of electromagnetic radiation, a paraxial beam is one that can be characterized by a small angular divergence, which is equivalent to saying that the angle between the optical axis $\hat{z}$ and a typical ray is small. The similarity between particle trajectories and optical rays runs even deeper than is suggested here, and we will see several other similar characteristics between paraxial particle and radiation beams in what follows.

In the first section we cover certain essential points regarding paraxial particle beams. We start by introducing the relativistic electron phase space, and continue with a very brief description of electron beam transport and linear particle optics. This discussion will be self-contained but rather incomplete, covering only those beam properties and dynamics that are required for subsequent study of X-ray generation from relativistic beams; interested readers can consult any of the numerous texts on accelerator physics, some of which we list in the References. We conclude this section with a brief introduction to the particle distribution function on phase space, which will be essential to the treatment of FEL dynamics in Chapters 3, 5, and 6.

The second section introduces paraxial wave optics, starting with a treatment of diffraction and certain geometrical optics that will parallel the particle beam physics from the previous section. We then place these similarities on more formal grounds by introducing phase space methods for wave optics, in which we define a quasi-distribution function for paraxial radiation that is analogous to the particle distribution function, with subtle but important differences that arise due to the wave nature of light. We conclude this section by discussing temporal coherence and its attendant intensity enhancement that is one of the distinctive features of laser light.

## 1.1 Particle (Electron) Beams

Our primary goal is to study radiation from highly relativistic electrons, by which we mean electrons whose speed $|\boldsymbol{v}|$ approaches the speed of light in vacuum. To get a handle on the approximate orders of magnitude involved, we first consider the electron energy $U_e = \gamma mc^2$, where $\gamma$ is the relativistic Lorentz factor, $m$ is the electron mass, and $c$

is the speed of light in vacuum. Thus, the Lorentz factor $\gamma$ is the ratio of the electron energy to its rest mass energy which, in terms of commonly used units, is given by

$$\gamma = \frac{U_e}{mc^2} = \frac{U_e[\text{GeV}]}{0.511 \times 10^{-3}} = 1957\, U_e[\text{GeV}]. \tag{1.1}$$

Typical FEL and synchrotron radiation sources use electron beams with energies from one to tens of GeV, so that $\gamma \sim 10^3$ to $10^4$. Additionally, if we define $\boldsymbol{\beta} \equiv \boldsymbol{v}/c$ to be the electron velocity scaled by the velocity of light $c$, the scaled speed $\beta \equiv |\boldsymbol{v}|/c$ is related to the Lorentz factor by

$$\beta = \sqrt{1 - \frac{1}{\gamma^2}} \approx 1 - \frac{1}{2\gamma^2}, \tag{1.2}$$

and

$$1 - \beta \approx 5 \times 10^{-8} \text{ for } \gamma mc^2 = 1.5 \text{ GeV}. \tag{1.3}$$

Thus, the electron speed approaches that of light to within a factor less than or of order $10^{-7}$. While it might therefore be tempting to approximately set $\beta \to 1$ from the beginning, we will see that certain essential radiation physics result from the fact that the electron speed is less than the speed of light $c$; mathematically, these effects typically appear as terms $\sim (1-\beta)^{-1}$. Therefore, we will have to take care to set $\beta \to 1$ only once we are sure that it is safe to do so.

### 1.1.1 Electron Beam Phase Space

The accelerating phase of modern radio-frequency (rf) accelerators typically accommodates tens to thousands of pico-Coulombs of charge, or $10^7$ to $10^{10}$ individual electrons. We will refer to this collection of electrons as an electron beam or bunch, so that an electron bunch is composed of $N_e \gg 1$ electrons whose relativistic velocity is primarily directed along $\hat{z}$. To describe this beam, it is convenient to adopt $z$, the propagation distance along a reference trajectory, as the independent variable or evolution parameter. This convention matches that of usual accelerator physics in the straight sections we study. We denote derivatives with respect to $z$ with a prime; for example,

$$x' \equiv \frac{dx}{dz} = \frac{dx/dt}{dz/dt} = \frac{1}{v_z}\frac{dx}{dt}. \tag{1.4}$$

Additionally, we will find that the physics of X-ray production are such that the transverse motion is largely independent of the longitudinal degrees of freedom. Hence, we employ the notation

$$\boldsymbol{x} \equiv (x, y) \qquad\qquad \boldsymbol{x}' \equiv (x', y')$$

for the transverse coordinates. For the relativistic paraxial beams that we consider, $x'$, $y' \ll 1$, and

$$|\boldsymbol{x}'| = \sqrt{x'^2 + y'^2} \approx \frac{1}{c}\sqrt{v_x^2 + v_y^2} \ll 1 \tag{1.5}$$

is the angle between $\hat{z}$ and the electron's velocity vector.

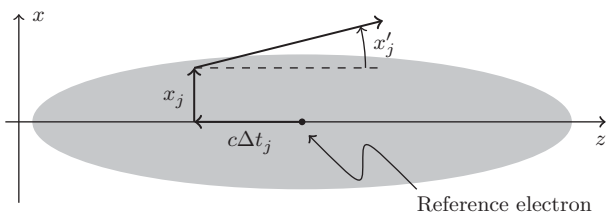


**Figure 1.1** Schematic representation of the transverse and longitudinal phase space variables of electrons in a bunch.

To fully describe the electron dynamics requires six independent phase space coordinates for every electron (three "positions" and three "momenta"), each of which is a function of the independent variable $z$. We further divide this phase space into transverse and longitudinal (or temporal) degrees of freedom. The transverse phase space variables are $(\boldsymbol{x}_j, \boldsymbol{x}'_j)$, where $\boldsymbol{x}_j = (x_j, y_j)$ are the transverse coordinates of the $j$th electron relative to the reference trajectory, while $\boldsymbol{x}'_j = (x'_j, y'_j)$ denote the transverse angles or divergence with respect to the $z$ axis, and $j = 1, 2, \ldots, N_e$. The longitudinal/temporal phase space variables are given by $(\Delta t_j, \Delta\gamma_j)$, where $\Delta t_j$ is the time that the electron arrives at the transverse plane located at $z$ relative to the nominal electron bunch time, and the energy deviation $\Delta\gamma_j \equiv \gamma_j - \gamma_0$ is defined with respect to the central beam energy $\gamma_0 mc^2$. We show the meaning of these coordinates in Figure 1.1. Note in particular that an electron with $\Delta t < 0$ arrives at a particular $z$ before the reference electron; in many cases it is more natural to use a longitudinal coordinate proportional to $-\Delta t$, since $(x, y, -\Delta t)$ form a right-hand coordinate system moving with the beam.[1]

### 1.1.2 Beam Transport and Linear Optics

The transport and control of particle beams is the purview of accelerator physics, and here we will only take a cursory look at certain transformations of transverse phase space for paraxial beams; more complete discussions of the physics of charged particle transport can be found in, e.g., [1, 2]. To simplify matters, we use the fact that the coordinates $\boldsymbol{x}$ and $\boldsymbol{x}'$ are small, and consider only those forces that are linear in $(\boldsymbol{x}, \boldsymbol{x}')$. In this case, the coordinates at the output plane $(\boldsymbol{x}, \boldsymbol{x}')_{\text{out}}$ can be written as linear combinations of the initial coordinates $(\boldsymbol{x}, \boldsymbol{x}')_{\text{in}}$ at the input plane. Thus, there exists a transformation matrix $\mathsf{M}$ that relates the two; for example, if the motion along $x$ is decoupled from that along $y$, we have

$$\begin{bmatrix} x \\ x' \end{bmatrix}_{\text{out}} = \mathsf{M}_{z_{\text{in}} \to z_{\text{out}}} \begin{bmatrix} x \\ x' \end{bmatrix}_{\text{in}} . \tag{1.6}$$

Furthermore, we will be specifically interested in straight transport sections that are composed of drift spaces where the beam propagates essentially in vacuum, interrupted by quadrupole magnets that provide transverse focusing. For free space propagation over a length $\ell$, we have the transformation

[1] Furthermore, in the Hamiltonian formulation $(-ct, mc\gamma)$ are canonical position–momentum conjugates; see Appendix A.

$$(x, x') \rightarrow (x + \ell x', x'), \tag{1.7}$$

which in matrix form is written as

$$\begin{bmatrix} x \\ x' \end{bmatrix}_{\text{out}} = \begin{bmatrix} 1 & \ell \\ 0 & 1 \end{bmatrix} \begin{bmatrix} x \\ x' \end{bmatrix}_{\text{in}} \equiv \mathsf{M}_\ell \begin{bmatrix} x \\ x' \end{bmatrix}_{\text{in}}. \tag{1.8}$$

A magnetic quadrupole acts like a focusing element which, under the thin-lens approximation, gives an electron a sudden change in angle (or "kick") that is proportional to its displacement from the axis. In the two planes we have the transformation rules

$$(x, x') \rightarrow (x, x' - x/f) \qquad (y, y') \rightarrow (y, y' + y/f). \tag{1.9}$$

We see that if the quadrupole focuses the beam in the $x$ direction, it is defocusing along $y$. The $4 \times 4$ matrix representation of (1.9) is

$$\begin{bmatrix} x \\ x' \\ y \\ y' \end{bmatrix}_{\text{out}} = \mathsf{M}_f \begin{bmatrix} x \\ x' \\ y \\ y' \end{bmatrix}_{\text{in}} = \begin{bmatrix} 1 & 0 & 0 & 0 \\ -1/f & 1 & 0 & 0 \\ 0 & 0 & 1 & 0 \\ 0 & 0 & 1/f & 1 \end{bmatrix} \begin{bmatrix} x \\ x' \\ y \\ y' \end{bmatrix}_{\text{in}}, \tag{1.10}$$

where we note that this matrix can be decomposed into two independent $2 \times 2$ blocks, one for each transverse direction.

In general, the total transport matrix of a beam line is obtained via the matrix multiplications of all the individual elements in the appropriate order. For $N$ elements numbered sequentially $n = 1, 2, \ldots, N$ (so that the beam first passes through element 1, than 2, etc.), the total transformation is given by

$$\mathsf{M} = \mathsf{M}_N \, \mathsf{M}_{N-1} \, \ldots \, \mathsf{M}_2 \, \mathsf{M}_1. \tag{1.11}$$

To conclude this section, we note that an equivalent and complementary description of linear beam transport can be formulated in terms of solutions to the linear differential equation

$$x'' + K(z)x = 0, \tag{1.12}$$

where $K(z)$ is an arbitrary function of $z$ whose form depends upon the linear element under consideration. For example,

$$K(z) = \begin{cases} 0 & \text{for free space propagation} \\ +\dfrac{\delta(z)}{f} & \text{for a focusing thin lens.} \end{cases} \tag{1.13}$$

It is easy to see that this formulation is equivalent to (1.7) and (1.9).

### 1.1.3 Beam Emittance and Envelope Functions

Tracking the millions to trillions of individual particle orbits in an electron beam requires significant computational resources. Often we are not even interested in the individual particle trajectories, but rather wish to know the overall "beam" properties that we can

easily measure. We express these beam properties as averages (or moments) of products of the transverse coordinates over the beam. If we orient our coordinate axes such that the average motion is along $\hat{z}$, the first-order moments vanish:

$$\langle x\rangle \equiv \frac{1}{N_e}\sum_j x_j = 0 = \langle x'\rangle \equiv \frac{1}{N_e}\sum_j x'_j. \tag{1.14}$$

In this case, the simplest beam properties are the second-order moments. Restricting ourselves to one transverse dimension for simplicity, the second-order beam moments have the following physical interpretation:

The squared RMS beam size:
$$\sigma_x^2(z) = \left\langle x^2\right\rangle = \frac{1}{N_e}\sum_j x_j^2. \tag{1.15}$$

The squared RMS beam angular divergence:
$$\sigma_{x'}^2(z) = \left\langle x'^2\right\rangle = \frac{1}{N_e}\sum_j x_j'^2. \tag{1.16}$$

The RMS beam correlation:
$$\left\langle x\,x'\right\rangle = \frac{1}{N_e}\sum_j x_j x'_j. \tag{1.17}$$

We further illustrate some example beam distributions using ellipses in phase space in Figure 1.2, showing the RMS size, divergence, and correlation. These ellipses are particularly convenient because they remain ellipses under linear transport, with phase space area proportional to the *geometric emittance* (or simply the emittance) defined by

$$\varepsilon_x \equiv \sqrt{\langle x^2\rangle\langle x'^2\rangle - \langle xx'\rangle^2}. \tag{1.18}$$

Since phase space area is conserved, the emittance (1.18) is an invariant of the linear transport lattice.[2]

The geometric emittance quantifies the phase space area occupied by an electron beam, with (1.18) specifying how much one must increase the RMS size to decrease the divergence and vice versa. As such, $\varepsilon_x$ gives an invariant measure of the beam quality

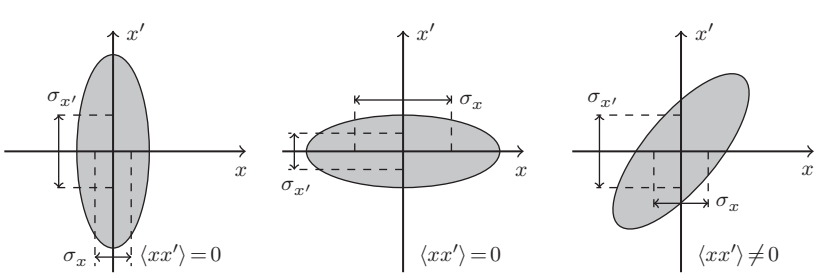


**Figure 1.2** Representative phase space ellipses, each of which have the same emittance $\varepsilon_x$. Note that either the beam size or divergence is minimized when the correlation $\langle xx'\rangle$ vanishes.

[2] While every Hamiltonian system conserves phase space area, nonlinear forces do not generically map initial ellipses to final ellipses in phase space. For this reason, $\varepsilon_x$ as defined in (1.18) is only invariant for linear forces. Additionally, generalizations to (1.18) are required if the linear forces couple motion in the $x$ direction to that along $y$ (or $t$).

which serves as an important metric for how the electron beam couples to the radiation. Since the FEL interaction typically puts a minimum requirement on the beam emittance, we might also like to know what beam quality we require from the injector at the beginning of the accelerator. However, acceleration will change the emittance $\varepsilon_x$ even if the transverse forces are linear. This is because our transverse coordinates $(\boldsymbol{x}, \boldsymbol{x}')$ are not canonically conjugate variables when $\gamma$ varies, so that the usual area conservation theorems of Hamiltonian mechanics do not apply in the space spanned by $(\boldsymbol{x}, \boldsymbol{x}')$. If we instead adopt the Hamiltonian position and momentum pair $(\boldsymbol{x}, \boldsymbol{p} = mc\beta_z\gamma\boldsymbol{x}')$, we can construct the *normalized emittance* $\varepsilon_{x,n}$ in a manner analogous to (1.18), with the property that $\varepsilon_{x,n}$ ideally remains invariant from the injector through the accelerating stages to the final insertion device. The value of the normalized emittance is related to the usual geometric emittance via

$$\varepsilon_{x,n} = \beta_z\gamma\varepsilon_x \approx \gamma\varepsilon_x. \tag{1.19}$$

The normalized emittance $\varepsilon_{x,n}$ is conserved through a linear system including acceleration, and is therefore often used as an important criterion for the beam produced by an electron gun.

Returning to the particle beam phase space with its transverse moments and geometric emittance $\varepsilon_x$, we introduce certain electron beam envelope functions that conveniently describe the beam properties. These envelope functions, which are referred to as the Courant–Snyder or Twiss parameters in the accelerator community, are usually defined as

$$\beta_x = \frac{\langle x^2\rangle}{\varepsilon_x} \qquad \gamma_x = \frac{\langle x'^2\rangle}{\varepsilon_x} \qquad \alpha_x = -\frac{\langle xx'\rangle}{\varepsilon_x}. \tag{1.20}$$

Although we typically reserve $\beta$ for the normalized electron velocity and $\gamma$ for its relativistic Lorentz factor, the notation (1.20) has been universally accepted and so we adopt it too; we will try to be clear when we are discussing the envelope functions. In view of the definition of the emittance (1.18), we have

$$\beta_x\gamma_x - \alpha_x^2 = 1, \tag{1.21}$$

and furthermore the Equations (1.20) also imply that

$$\frac{d\beta_x}{dz} = -2\alpha_x. \tag{1.22}$$

Beam emittance and the envelope functions, especially the beta function $\beta_x$, are the everyday concern of accelerator physicists, with $\beta_x$, $\gamma_x$, and $\alpha_x$ typically regarded as properties of the beam line or optical lattice. The emittance is a property of the beam that characterizes its quality, while the physical size and divergence are determined by both the beam and the lattice properties.

### 1.1.4 Beam Properties under Simple Transport

Now, we investigate the beam envelope functions and the RMS moments in two simple but physically important situations. First, we consider electron transport through

free space, after which we study beam evolution in a focusing lattice comprised of periodically spaced quadrupoles.

### Free Space Transport

We calculate the free space transport of a beam over a distance $z$ using the matrix (1.8) with $\ell = z$, writing

$$\begin{bmatrix} x \\ x' \end{bmatrix}_{\text{out}} = \begin{bmatrix} 1 & z \\ 0 & 1 \end{bmatrix} \begin{bmatrix} x \\ x' \end{bmatrix}_{\text{in}}. \tag{1.23}$$

Thus, the evolution of the RMS beam size is given by

$$\left\langle x_{\text{out}}^2 \right\rangle = \left\langle \left(x_{\text{in}} + z x'_{\text{in}}\right)^2 \right\rangle = \left\langle x_{\text{in}}^2 \right\rangle + 2z \left\langle x_{\text{in}} x'_{\text{in}} \right\rangle + z^2 \left\langle x'^2_{\text{in}} \right\rangle, \tag{1.24}$$

while the divergence is constant, $\sigma_{x'}(z) = \sigma_{x'}(0)$. If we assume that the initial correlation is zero (i.e., that $\langle x_{\text{in}} x'_{\text{in}} \rangle = 0$) and apply the definitions (1.20), we obtain

$$\beta_x(z) = \beta_x(0) + z^2 \gamma_x(0). \tag{1.25}$$

Since we have assumed that there is initially no correlation, $\alpha_x(0) = 0$ and the identity (1.21) implies that $\gamma_x(0) = 1/\beta_x(0)$. Thus, we have

$$\beta_x(z) = Z_\beta + \frac{z^2}{Z_\beta}, \tag{1.26}$$

where the focusing parameter[3] $Z_\beta = \beta_x(0)$ is determined by the focusing conditions outside the drift space. The RMS beam size is given by

$$\sigma_x(z) = \sqrt{\varepsilon_x \beta_x(z)} = \sqrt{\varepsilon_x \left( Z_\beta + \frac{z^2}{Z_\beta} \right)}. \tag{1.27}$$

The RMS size is a minimum at $z = 0$ when the correlation vanishes; this location is known as the beam waist. At small longitudinal distances the beam expands quadratically with $z$, while the beam size increases linearly if $z \gg Z_\beta$. This beam spreading occurs because different particles travel at different angles even though each individual particle trajectory is a straight line, as shown in Figure 1.3.

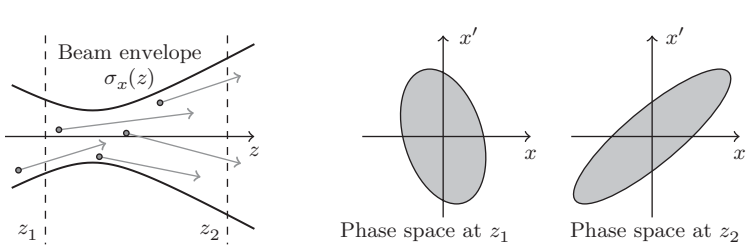


**Figure 1.3** Illustration of straight electron trajectories giving rise to a diverging beam envelope. On the left are several electron trajectories and the free-space beam size in the $x$-$z$ plane. On the right we draw the phase space ellipses in the $(x, x')$ plane at position $z_1$ and $z_2$.

[3] Particle collider physicists typically use $\beta_x^*$ to denote our $Z_\beta$.

## Alternating Gradient Focusing Lattice

We now consider a simple focusing lattice consisting of a periodic series of quadrupoles and drift spaces. Since a quadrupole only focuses in one plane at a time (i.e., either $x$ or $y$), one typically achieves focusing in both planes by using a lattice whose elementary cell consists of two quadrupoles separated by drift sections as shown in Figure 1.4. The first quad focuses the beam in the $x$ direction while it defocuses in $y$, and the second quad is defocusing in $x$ while focusing in $y$. The net effect of the focusing-drift–defocusing-drift (FODO) lattice is to confine the beam in both directions, which can be seen from the phase space diagrams in Figure 1.4.

For high-gain FELs, one typically wants small variations in the beam size (or $\beta_x$-function) while minimizing the angular divergence (the $\gamma_x$-function). This can be done by using a particular FODO lattice whose phase space transformations are shown pictorially in Figure 1.4. Note how the projection on the $x$ axis has small variations, while the projection on the $x'$ axis is small at all times. Physically, this focusing lattice uses lenses whose focal lengths are much longer than the drift space distance, with $|f| \gg \ell$.

The FODO lattice can be simply analyzed if we consider the input and output planes to be "halfway" through the first focusing quad shown in Figure 1.4. In this case, the correlation $\langle xx' \rangle$ is zero at the input and output planes as indicated in the figure. Since the focal length of one-half a lens is twice the focal length of the full lens (as can be seen through a matrix multiplication), the matrix transformation of one cell is given by

$$\begin{aligned} \mathsf{M}_{\text{FODO}} &= \begin{bmatrix} 1 & 0 \\ -1/2f & 1 \end{bmatrix} \begin{bmatrix} 1 & \ell \\ 0 & 1 \end{bmatrix} \begin{bmatrix} 1 & 0 \\ 1/f & 1 \end{bmatrix} \begin{bmatrix} 1 & \ell \\ 0 & 1 \end{bmatrix} \begin{bmatrix} 1 & 0 \\ -1/2f & 1 \end{bmatrix} \\ &= \begin{bmatrix} 1 - \frac{\ell^2}{2f^2} & 2\ell\left(1 + \frac{\ell}{2f}\right) \\ -\frac{\ell}{2f^2}\left(1 - \frac{\ell}{2f}\right) & 1 - \frac{\ell^2}{2f^2} \end{bmatrix}. \end{aligned} \tag{1.28}$$

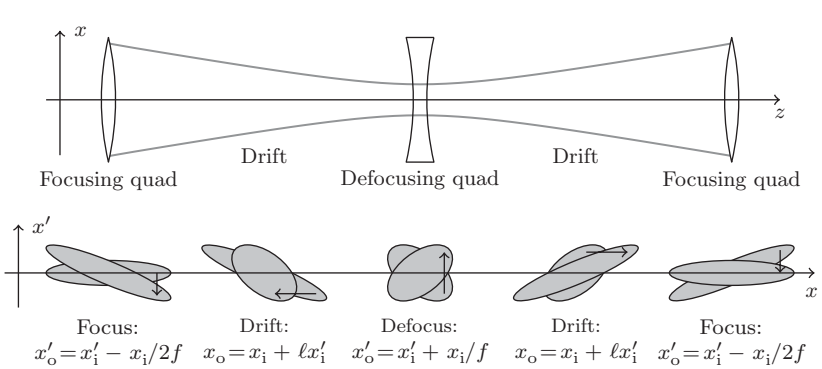


**Figure 1.4** The basic unit of a FODO lattice consists of a focusing quadrupole, drift space, defocusing quadrupole, and drift space. The top shows the unit cell of a FODO lattice that begins and ends at the symmetric point in the middle of the focusing quad, while the bottom shows the phase space transformations for the electron beam over this length. The defocusing transformation shown is across the entire quadrupole, so that in the middle of the magnet the beam is uncorrelated in $xx'$.

For periodic motion we have $\beta_x(0) = \beta_x(2\ell)$ and $\gamma_x(0) = \gamma_x(2\ell)$, while vanishing correlation $\alpha_x$ at the two planes implies that $\beta_x(0) = 1/\gamma_x(0)$ from (1.21). We compute the beam size in a manner similar to that done for free space propagation in (1.24); solving the resulting quadratic equation for $\beta_x(0)$, we find that

$$\beta_x(0) = 2\sqrt{\frac{2f^3 + f^2\ell}{2f - \ell}} \approx 2\,|f|\left(1 + \frac{\ell}{2f}\right) \tag{1.29}$$

for $f \gg \ell$. If we had set the input and output planes at consecutive defocusing quadrupoles the calculation would have been identical but with $f \to -f$, so that

$$\beta_x(\ell) \approx 2\,|f|\left(1 - \frac{\ell}{2f}\right). \tag{1.30}$$

Between the quadrupoles the beta-function is an approximately linear function of $z$, so that from Equation (1.22) we have $d\beta_x/dz = -2\alpha_x \approx -2$ in the first half-period, while $d\beta_x/dz = -2\alpha_x \approx +2$ in the second half-period. Nevertheless, in the limit $|f| \gg \ell$ the envelope functions $\beta_x$, $\gamma_x$, and $\alpha_x$ are approximately constant throughout the lattice. We could calculate the average $\gamma_x$-function in a manner similar to what we did for $\beta_x$, but it is simpler to apply the identity

$$\gamma_x = \frac{1 + \alpha_x^2}{\beta_x} \approx \frac{1}{|f|}, \tag{1.31}$$

where the final result follows from $\alpha_x \approx \pm 1$ and the formulas for $\beta_x$ above.

Now, we can write down the average values of the lattice functions for the FODO lattice in the limit $|f| \gg \ell$. Including the corresponding RMS beam size, divergence, and correlation, we have

$$\beta_x(z) \approx \bar{\beta}_x = 2f \qquad \to \qquad \left\langle x^2 \right\rangle \approx 2\varepsilon_x f \tag{1.32}$$

$$\gamma_x(z) \approx \frac{2}{\bar{\beta}_x} = \frac{1}{f} \qquad \to \qquad \left\langle x'^2 \right\rangle \approx \frac{\varepsilon_x}{f} \tag{1.33}$$

$$\alpha_x^2(z) \approx \bar{\beta}_x\bar{\gamma}_x - 1 = 1 \qquad \to \qquad \left\langle xx' \right\rangle \approx \pm\varepsilon_x. \tag{1.34}$$

Note how the envelope functions depend on only the lattice parameters $\ell$ and $f$ (in this approximation, they depend only on the focal strength $f$), while the physical size, divergence, and correlation also depend on the beam quality through the emittance $\varepsilon_x$.

### 1.1.5 Electron Distribution Function on Phase Space

We close our discussion of electron beams with a brief introduction to the electron distribution function in phase space. In general, we take the electron distribution function to be a nonnegative function $F$ of the phase space coordinates, whose value is proportional to the number of electrons per unit phase space volume. For example, in the previous section the ellipses of Figures 1.2 and 1.3 could be thought of as representing the distribution function in 4D transverse phase space, with the shaded areas proportional to the local density of electrons. In this simple idealization, the transverse distribution function is uniform inside the ellipse and zero outside.

A complete, classical description of the $N_e$ electrons in the bunch can be obtained by using the Klimontovich distribution function, which represents each point-like electron by a delta-function centered about its trajectory in 6D phase space:

$$F(\Delta t, \Delta\gamma, \boldsymbol{x}, \boldsymbol{x}'; z) = \frac{1}{N_e}\sum_{j=1}^{N_e} \delta[\Delta t - \Delta t_j(z)]\delta[\Delta\gamma - \Delta\gamma_j(z)] \times \delta[\boldsymbol{x} - \boldsymbol{x}_j(z)]\delta[\boldsymbol{x}' - \boldsymbol{x}'_j(z)]. \tag{1.35}$$

We choose the normalization so that integrating $F$ over all the coordinates is unity. Furthermore,

$$N_e F(\Delta t, \Delta\gamma, \boldsymbol{x}, \boldsymbol{x}'; z)\, d\boldsymbol{x} d\boldsymbol{x}' d(\Delta t) d(\Delta\gamma) \tag{1.36}$$

is the number of particles per unit phase space volume whose coordinates are in the 6-cube defined by the sides $(\boldsymbol{x}, \boldsymbol{x} + d\boldsymbol{x})$, $(\boldsymbol{x}', \boldsymbol{x}' + d\boldsymbol{x}')$, etc.

Conservative (Hamiltonian) dynamics transports the value of the distribution function along single particle trajectories. In this case $F$ behaves as an incompressible fluid in phase space that satisfies the Liouville equation

$$\frac{d}{dz}F = \left[\frac{\partial}{\partial z} + (\Delta t)'\frac{\partial}{\partial \Delta t} + (\Delta\gamma)'\frac{\partial}{\partial \Delta\gamma} + \boldsymbol{x}'\cdot\frac{\partial}{\partial \boldsymbol{x}} + \boldsymbol{x}''\cdot\frac{\partial}{\partial \boldsymbol{x}'}\right]F = 0. \tag{1.37}$$

Although the Klimontovich distribution function is a complete description and will be an important tool for analysis in subsequent chapters, it frequently contains more information than is physically required. Often, we can approximate the distribution as a smooth phase space fluid whose value is proportional to the local density. As we mentioned in the beginning of the section, the constant-valued density contained in the phase space ellipse is one such simplification (these types of constant distributions are often referred to as "waterbag" distributions). Another convenient distribution function that can be handled analytically is a Gaussian function. In fact, if the only things we know about $F$ are the first- and second-order moments (the former being zero, the latter being given by the envelope functions and $\varepsilon_x$), than a Gaussian $F$ is the distribution of maximum entropy, and hence is the best we can do with the given information.[4]

As mentioned previously, for X-ray generation the transverse electron dynamics typically does not depend on the longitudinal physics, so that we can consider the transverse distribution function independently of the longitudinal distribution. Subsequent chapters mainly focus on the longitudinal dynamics relevant to radiation generation and the FEL interaction, while here we introduce some general concepts that, in keeping with our prior discussion, we apply to the transverse part of $F$. We introduce the Gaussian phase space distribution in one transverse dimension for simplicity, as extension to 2D is trivial. Assuming a Gaussian transverse distribution function whose second-order moments are consistent with the envelope functions (1.20) implies that

$$F(x, x'; z) = \frac{1}{2\pi\varepsilon_x}\exp\left\{-\frac{1}{2\varepsilon_x}\left[\gamma_x(z)x^2 + \beta_x(z)x'^2 + 2\alpha_x(z)xx'\right]\right\} \tag{1.38}$$

[4] If higher-order moments of $F$ are known, than an appropriate distribution consistent with this data should be chosen.